Binding modes of 6,7 di-substituted 4-anilinoquinoline-3-carbonitriles to EGFR

Nagaraju Akula,[a] Jag Bhalla,[b,†] Jayalakshmi Sridhar[a,†] and Nagarajan Pattabiraman[a,b,*]

[a]*Department of Oncology, Lombardi Comprehensive Cancer Center, Georgetown University, Washington, DC 20057, USA*
[b]*Department of Biochemistry and Molecular Biology, Georgetown University, Washington, DC 20057, USA*

Abstract—4-Anilino-3-cyanoquinolines were reported to have irreversible binding to epidermal growth factor receptor kinase (EGFRK) by forming a covalent linkage to C773. Our initial docking studies gave results inconsistent with the in vitro data and showed two different binding modes. To perceive the exact mode of binding of these ligands, two models of the ligand–EGFR complexes were considered: (1) reversible binding mode in which the ligand had hydrogen bond interactions at the binding site and (2) irreversible binding mode wherein the ligand's Michael acceptor side chain has proximity to the sulfhydryl group of C773 of EGFR, thereby enabling a covalent interaction. The irreversible binding mode correlated better than reversible binding mode with respect to in vitro data. However, our results indicate that both modes are being adopted by the ligands and could be utilized to design more potent EGFRK inhibitors.
© 2004 Elsevier Ltd. All rights reserved.

1. Introduction

EGFR belonging to the group-I receptor tyrosine kinases plays a key role in vital signal transduction pathways responsible for cell division and differentiation.[1] Overexpression and deregulated expression of EGFR has been observed as a feature of uncontrolled cell proliferation leading to certain types of cancer.[2] Compounds that inhibit the kinase activity of EGFR are of potential interest as therapeutic antitumor agents.[3,4] Recently, a new class of 4-anilinoquinoline-3-carbonitriles has been reported as irreversible EGFR tyrosine kinase inhibitors.[5] Their basic pharmacophore was modified with the help of docking studies using a homology model of EGFR, wherein an irreversible interaction between the Michael acceptor side chain of the inhibitor and the sulfhydryl hydrogen of C773 was indicated.[5,6] Later, the crystal structure of the kinase domain of EGFR with 4-anilinoquinazoline was described by Stamos et al.,[7] wherein the authors found the binding of quinazoline to EGFRK differed in detail from previous homology modeling studies.[8] The inhibitor utilized for the crystal structure did not have the structural moiety capable of making covalent linkage to C773. In our quest to understand this novel irreversible binding of the ligand to the C773 residue of the kinase, we carried out molecular docking studies. Our initial FlexiDock and Dock studies of the series of 4-anilino-quinoline-3-carbonitriles indicated that most of the ligands preferred to dock at the binding site. Only a few oriented in such a manner, that the Michael acceptor was easily accessible for a covalent linkage with the C773 residue. The docking scores also did not correlate to the in vitro data. It became clear from these studies that these ligands cannot satisfy both the conditions of formation of a covalent linkage with the sulfhydryl group of C773 and also hydrogen bond interactions at the binding site as reported. To better understand the exact mode of binding of these ligands to EGFR, two models were considered and molecular minimization studies were carried out. The first model (reversible binding mode) had the ligands oriented as in the crystal structure[7] and the second model (irreversible binding mode) had ligands oriented with the Michael acceptor at such a distance from the sulfhydryl group of C773 so as to favor a covalent linkage. Binding energies and scoring functions of the minimized complexes of both the models were analyzed.

2. Computational methodology

All ligands were designed using the sketcher module of Sybyl6.9 (Tripos Associates, St. Louis, MO) on a Silicon Graphics Octane2 workstation. Initial geometric optimizations were carried out using the standard MMFF94 force field, with a 0.001 kcal/mol energy gradient convergence criterion and a distance-dependent dielectric constant employing Gasteiger charges. Further geometric optimizations were performed using the semi-empirical method Molecular Orbital Package (MOPAC).[9] Molecular minimizations of the ligand–protein complexes were carried out using Sybyl6.9. The protein–ligand complex was constructed based on the X-ray structure (PDB entry 1M17) and these complexes were minimized by using MMFF94 Force Field until the iteration number reached 5000. The scoring functions (D-Score, G-Score, Chem-Score, and PMF-Score) of ligands were calculated from minimized ligand protein complex by using Cscore[10–13] of Sybyl6.9.

3. Results and discussion

Initial docking studies could not give a clear understanding of the binding mode of the ligands, hence manually docked complexes were built and studied. In the reversible binding mode studies each ligand was docked at the bound ligand (Erlotinib) position with same orientation of crystal structure in order to cover the binding pocket and minimized the ligand–protein complex. In irreversible binding mode, the ligand molecules were manually placed close to C773 with orientation towards binding pocket and minimized by giving a 3 Å distance constraint in between the β-carbon of the ligand to cysteine.
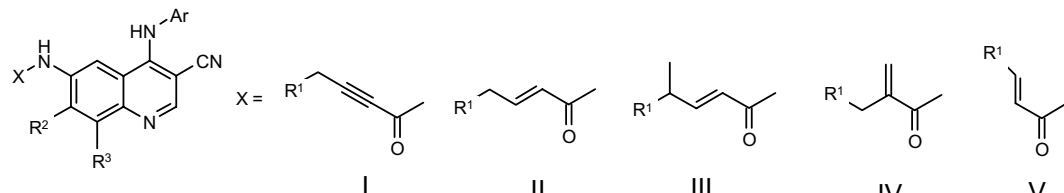
3.1. Reversible binding mode

After docking and minimization, it was observed that most of the ligands with good binding energy retained the crystal structure ligand orientation. A few of the ligands with poor binding energy moved away from the crystal structure ligand orientation. The poor binding energy ligands were reported to have low in vitro activity (IC_{50}). The most active ligand **5** not only showed good binding energy but also maintained the N–H···[1]N intermolecular H-bonding interaction with M769 and O–H···[3]N interaction of the 3-cyano group with the Thr766 of the protein as exhibited by the crystal structure ligand. But the distance between the Michael acceptor side chain and the sulfhydryl group of the C773 of the protein was 5.97 Å, which is more than the permissible distance for a covalent linkage. The nitrogen atom of the dimethyl amino group was at a distance of 7 Å from the C773 sulfhydryl group (Fig. 1a). The least active ligand **41** exhibited poor binding energy as well as a shift in the position of the ligand while maintaining the hydrogen bond interactions with M769 and T766. The distance from the Michael acceptor side chain of **41** and the C773 residue of the protein was found to be 6.6 Å and the nitrogen atom of the dimethyl amino group was 8.1 Å from C773 (Fig. 1b). The correlation of the binding energy with the in vitro activity data was 0.50 (Table 1) and the evaluated Cscore functions did not correspond well to the in vitro data.

3.2. Irreversible binding mode

Mutation studies (C773S) by Fry et al.[14] showed that PD168393 specifically interacted with the sulfhydryl group of C773 in an irreversible manner. A similar interaction was suggested by Wissner et al.[5] Minimized protein–ligand complex structures in the irreversible binding mode were generated for all the ligands and
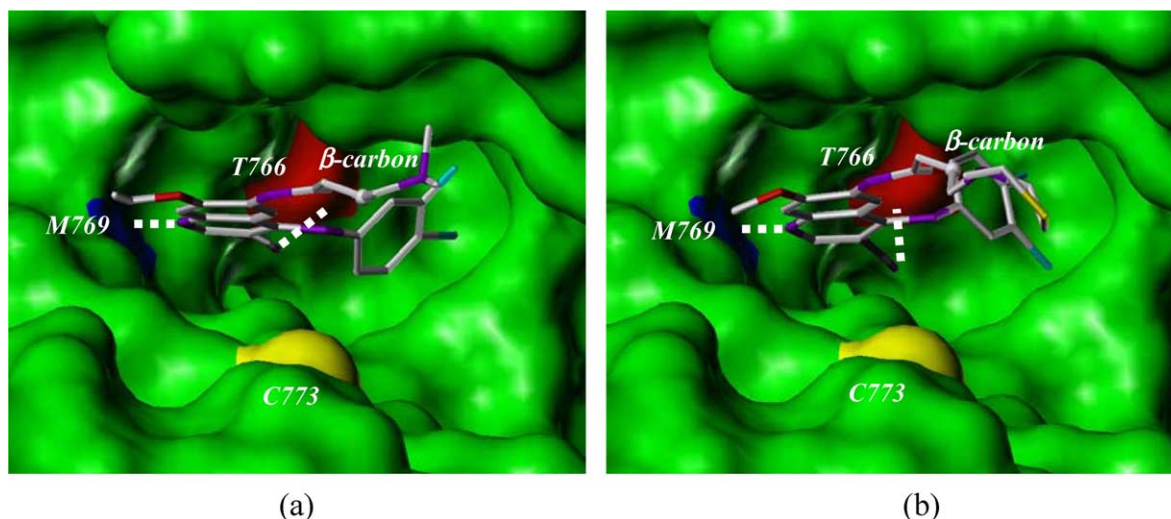
Figure 1. Minimized reversible binding mode of the ligand–EGFR complexes (a) ligand 5 and (b) ligand 41. EGFR protein binding sites are represented by molecular surfaces generated by MOLCAD (blue color indicates N of M769, red indicates O of T766 and yellow indicates S of C773) and the bound ligands represented as stick models. Dotted lines represent hydrogen-bonding interactions with the M769 and T766 of EGFR.

Table 1. Binding energies (BE) for the minimized reversible (RB) and irreversible (IRB) ligand–EGFR complexes


Ligand (series)	R^1	R^2	R^3	Ar	IC_{50}[a]	BE (RB)	BE (IRB)
5 (II)	$N(CH_3)_2$	OC_2H_5	H	3-Cl, 4-Fl	0.08	−253.1	−251.5
18 (I)	H	H	H	3-Br	0.94	−222.4	−195.7
19 (I)	OCH_3	H	H	3-Br	0.96	−164.5	−287.1
20 (I)	$O(CH_2)_2OCH_3$	H	H	3-Br	0.93	−139.5	−210.1
21 (I)	OCH_2OCH_3	H	H	3-Br	0.33	−173.5	−234.5
22 (I)	Thiomorpholinyl	H	H	3-Br	0.55	−323.5	−236.4
23(I)	2(S)-2-(methoxymethyl-1-pyrrolidinyl)	H	H	3-Br	0.15	−225.0	−194.3
24 (I)	$N(n\text{-}Pr)_2$	H	H	3-Br	0.13	−200.0	−228.2
25 (I)	$N(i\text{-}Pr)_2$	H	H	3-Br	0.25	−296.0	−221.9
26 (I)	H	OCH_3	H	3-Br	0.91	−303.4	−209.5
27 (I)	OCH_3	OCH_3	H	3-Br	0.79	−239.8	−244.6
28 (I)	$N(CH_3)_2$	OCH_3	H	3-Br	0.09	−235.9	−250.5
30 (II)	$N(CH_3)_2$	H	H	3-Br	0.31	−232.9	−178.7
31 (II)	$N(CH_3)_2$	OCH_3	H	3-Br	0.79	−189.0	−213.7
32 (II)	N-morpholinyl	OCH_3	H	3-Br	3.83	−193.0	−218.1
33 (II)	$N(CH_3)_2$	OC_2H_5	H	3-Br	1.6	−211.5	−40.6
34 (II)	N-morpholinyl	OC_2H_5	H	3-Br	10.3	−13.0	116.3
35 (II)	$N(CH_3)_2$	H	OCH_3	3-Br	2.88	−173.7	3.8
36 (II)	N-morpholinyl	H	OCH_3	3-Br	5.39	−133.1	−116.6
37 (II)	$N(CH_3)_2$	H	H	3-Cl, 4-F	0.65	−125.0	−251.5
38 (II)	N-morpholinyl	H	H	3-Cl, 4-F	2.29	−219.3	9.6
39 (II)	$N(CH_3)_2$	OCH_3	H	3-Cl, 4-F	2.32	−161.9	−7.5
40 (II)	$N(C_2H_5)_2$	OCH_3	H	3-Cl, 4-F	1.91	−223.4	−99.8
41 (II)	N-morpholinyl	OCH_3	H	3-Cl, 4-F	13.6	−143.7	94.5
42 (II)	$N(CH_3)_2$	H	H	3-Cl, 4-F	2.64	−197.5	66.7
43 (III)	$N(CH_3)_2$	OCH_3	H	3-Cl, 4-F	5.22	−167.7	−38.3
44 (III)	$N(C_2H_5)_2$	OCH_3	H	3-Cl, 4-F	4.84	−236.5	19.9
45 (III)	N-morpholinyl	OCH_3	H	3-Cl, 4-F	10.6	−119.6	−102.6
47 (V)	H	H	H	3-Br	0.59	−157.5	−196.2
48 (V)	H	OCH_3	H	3-Br	0.81	−93.4	−201.1
49 (V)	CH_3	H	H	3-Br	1.62	−107.1	−155.8
50 (V)	CH_3	OC_2H_5	H	3-Cl, 4-F	7.5	−89.4	−125.4
51 (IV)	N-morpholinyl	H	H	3-Cl, 4-F	2.7	−115.9	−203.0
52 (IV)	$N(CH_3)_2$	OC_2H_5	H	3-Cl, 4-F	0.56	−149.9	−224.3
Correlation						0.5	0.7

[a] IC_{50} values are in µM concentrations (taken from Ref. 5).

their binding energy calculated. In these structures, most of the ligands moved away from the binding site, while maintaining the covalent linkage. The most active ligand **5** also moved out of the pocket resulting in a loss of the hydrogen bonding interactions. The orientation of **5** appeared to cap the entry space of the binding pocket (Fig. 2a). The least active ligand **41** also moved away from the binding pocket accompanied by the loss of hydrogen bonding interactions with the binding site; it oriented itself so as to partially cover the access to the binding pocket (Fig. 2b). It could be clearly seen from this study that when the ligand formed a covalent linkage with the C773, it could not occupy the binding site in its entirety. The reason for the in vitro activity of some of these ligands could be because of the inaccessibility of the binding pocket for ATP. The correlation of calculated binding energies with the in vitro data was 0.70

(Table 1), significantly better than what was obtained by reversible docking and minimization. It is interesting to note that the PMF score from the Cscore evaluations for irreversible binding mode showed correlation of 0.50 to the activity data.

Our studies indicate that the both irreversible and reversible binding modes can be adopted by the ligands. As the correlation values of binding energies with in vitro data of reversible and irreversible binding modes are in close proximity, they could indicate that all the ligands are not binding in the same manner. They also depict the different orientations that the ligands could adopt in the binding pocket. Even though these differences are dramatic, the ligands seem to be acting as chemical modifiers of EGFR thereby preventing ATP from reaching the binding pocket. Designing a
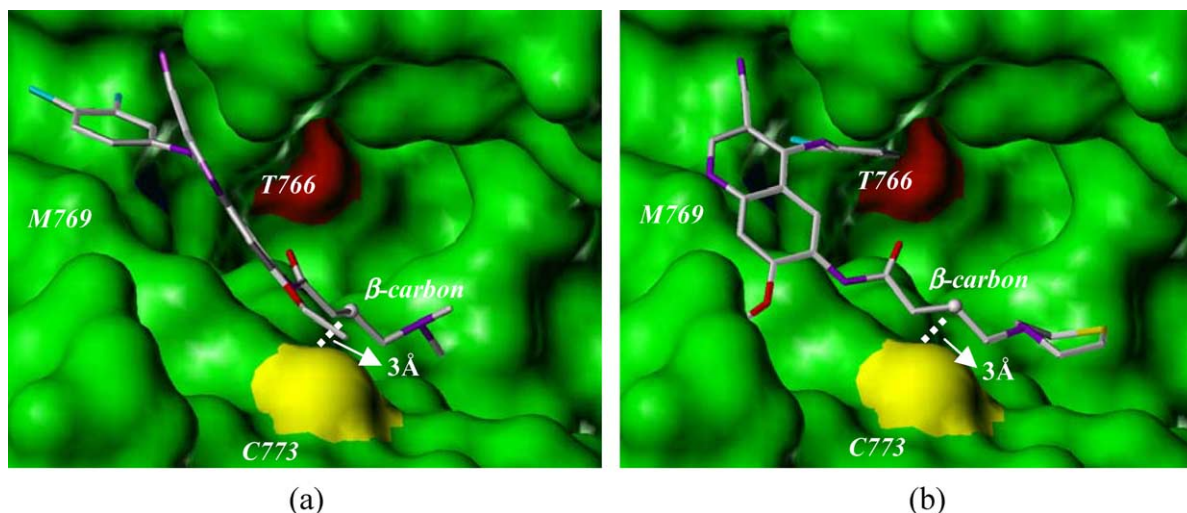
Figure 2. Minimized irreversible binding mode of the ligand–EGFR complexes (a) ligand 5 and (b) ligand 41. EGFR protein binding sites are represented by molecular surfaces generated by MOLCAD (blue color indicates N of M769, red indicates O of T766 and yellow indicates S of C773) and the bound ligands represented as stick models. The dotted lines depict the distance between the β-carbon atom of the Michael acceptor side chain and Sγ atom of C773.

compound that could occupy the binding pocket completely, make the hydrogen bonding interactions at the binding site and also form a covalent linkage with the sulfhydryl group of C773 could result in a very potent inhibitor of EGFR.

References and notes

1. Schlessinger, J.; Ullrich, A. *Neuron* **1992**, *9*, 383–391.
2. Hunter, T. *Cell* **2000**, *100*, 113–127.
3. Bridjes, A. J. *Curr. Med. Chem.* **1999**, *6*, 825–843.
4. Boschelli, D. H. *Drugs Future* **1999**, *24*, 515–537.
5. Wissner, A.; Overbeek, E.; Reich, M. F.; Floyd, M. B.; Johnson, B. D.; Mamuya, N.; Rosfjord, E. C.; Discafani, C.; Davis, R.; Shi, X.; Rabindran, S. K.; Gruber, B. C.; Ye, F.; Hallet, W. A.; Nilakantan, R.; Shen, R.; Wang, Y.-F.; Greenberger, L. M.; Tsou, H.-R. *J. Med. Chem.* **2003**, *46*, 49–63.
6. Tsou, H.-R.; Mamuya, N.; Johnson, B. D.; Reich, M. F.; Gruber, B. C.; Ye, F.; Nilakantan, R.; Shen, R.; Discafani, C.; DeBlanc, R.; Davis, R.; Koehn, F. E.; Greenberger, L. M.; Wang, Y.-F.; Wissner, A. *J. Med. Chem.* **2001**, *44*, 2719–2734.
7. Stamos, J.; Sliwkowski, M. X.; Eigenbrot, C. *J. Biol. Chem.* **2002**, *277*, 46265–46272.
8. Wissner, A.; Berger, D. M.; Boschelli, D. H.; Floyd, M. B.; Greenberger, L. M.; Gruber, B. C.; Johnson, B. D.; Mamuya, N.; Nilakantan, R.; Reich, M. F.; Shen, R.; Tsou, H. R.; Upeslacis, E.; Wang, Y. F.; Wu, B. Q.; Ye, F.; Zhang, N. *J. Med. Chem.* **2000**, *43*, 3244–3256.
9. Besler, B. H.; Merz, K. A.; Kollman, P. A. *J. Comp. Chem.* **1990**, *11*, 431–439.
10. Meng, C.; Shoichet, B. K.; Kuntz, I. D. *J. Comp. Chem.* **1992**, *13*, 505–524.
11. Muegge, I.; Martin, Y. C. *J. Med. Chem.* **1999**, *42*, 791–804.
12. Eldridge, M. D.; Murray, C. W.; Auton, T. R.; Paolini, G. V.; Mee, R. P. *J. Comp-Aided Molec. Des.* **1997**, *11*, 425–445.
13. Bohm, H.-J. *J. Comp-Aided Molec. Des.* **1994**, *8*, 243–256.
14. Fry, D. W.; Bridges, A. J.; Denny, W. A.; Doherty, A.; Greis, K. D.; Hicks, J. L.; Hook, K. E.; Keller, P. R.; Leopald, W. R.; Loo, J. A.; McNamara, D. J.; Nelson, J. M.; Sherwood, V.; Smaill, J. B.; Trumpp-Kallmeyer, S.; Dobrusin, E. M. *Proc. Natl. Acad. Sci. U.S.A.* **1998**, *95*, 12022–12027.